Bioinspired nanocomposite films with graphene and MXene

Lei Li[a], Qunfeng Cheng[a,b,*]

[a] School of Chemistry, Key Laboratory of Bio-inspired Smart Interfacial Science and Technology of Ministry of Education, Beihang University, Beijing, 100191, P. R. China
[b] School of Materials Science and Engineering, Zhengzhou University, Zhengzhou, 450001, P. R. China

Two dimensional nanomaterials, such as graphene and MXene, have been widely used to fabricate high performance nanocomposite films owing to their unique structure and excellent physiochemical properties, showing enormous potential applications in many areas. However, the existing voids and wrinkling in the nanocomposite films inevitably impedes realizing the high performance of the nanocomposite films during the assembly process of graphene and MXene nanosheets. Nacre provides an inspiration for fabricating high performance graphene and MXene nanocomposite films through constructing a high alignment structure and strong interface interactions. In this review, we summarize the preparation approaches of graphene and MXene nanocomposite films and discuss the mechanical properties. Then, several effective strategies for assembling graphene and MXene nanosheets have been concluded and discussed. Meanwhile, we also summarize and discuss the applications of graphene and MXene nanocomposite films including electromagnetic interference (EMI) shielding and thermal management. Finally, outlooks and challenges are proposed to promote their progress and applications in the future.

1 Introduction

Since the first discovery of graphene in 2004, graphene has gradually aroused widespread attention [1]. Due to the outstanding mechanical, electrical and thermal properties, graphene has been applied in flexible electronic devices, aerospace and thermal management fields in the past decade [2–6]. For instance, the single-layer graphene has a Young's modulus of 1.0 TPa [7] and a superhigh thermal conductivity of about 5300 W/mK [8] at room temperature, demonstrating enormous practical potentiality in the above mentioned fields. Before realizing

these applications, it is crucial to assemble graphene nanosheets into high performance graphene nanocomposites including one dimensional (1D) fiber, two dimensional (2D) film and three dimensional (3D) bulk. Especially, high performance graphene nanocomposite films have gained enormous attention. However, it is difficult to achieve high performance nanocomposite films due to weak interaction between adjacent graphene nanosheets. Graphene oxide (GO) is a usual precursor for obtaining graphene with plentiful surface terminating groups, which can easily interact with various materials for preparing nanocomposite films [9,10]. Meanwhile, in recent years, MXene, a novel two dimensional (2D) materials, shows promising electrical and thermal properties, which shows promising application in aerospace field [11–16]. Indeed, compared with graphene, the intrinsic mechanical and thermal conductivity properties and

stabilities of MXene is relatively poor. Furthermore, the easily oxidizable characteristics and thermal vulnerability of MXene may restrict its practical applications. However, compared with graphene, MXene has plentiful surface functional groups, which is an ideal building block for fabricating nanocomposite films without chemical modification any more.

Since 2007, there have been many studies on graphene and MXene nanocomposite films [17–21]. Up to now, despite a great deal of works have been studied, the graphene and MXene nanocomposite films still exist great challenges for achieving high performance. For example, the voids have been formed inevitably during the assembly process, resulting in poor mechanical properties [22]. Moreover, the wrinkling of graphene and MXene nanosheets also leads to the lower mechanical and thermal properties of resultant nanocomposite films [23]. Hence, it still exists a great challenge to obtain outstanding mechanical properties and other functional properties simultaneously in graphene and MXene nanocomposite films.

Traditionally, the graphene and MXene nanocomposites are prepared by some strategies of solution mixing [24], melt mixing [25] and in-situ polymerization [26]. However, these obtained nanocomposites show poor performance due to the inferior alignment degree of filler nanosheets in polymer matrix and the existing weak interfacial interactions between filler nanosheets and polymer matrix. Over billions of years of evolution, many biological materials, such as nacre, bamboo and wood have developed their unique multiscale structures with outstanding properties [27–29]. Particularly, nacre is a typical organic-inorganic nanocomposite, which is consisted of 95 vol% aragonite flakes and 5 vol% organic biopolymers [30]. Owing to the typically well-aligned layered structure and plentiful interface interactions, nacre shows superior mechanical properties, which provides an inspiration for preparing high performance nanocomposites based on 2D nanosheets.

Herein, we first conclude and classify the preparation methods of graphene and MXene nanocomposite films. Subsequently, we discuss the mechanical properties of graphene and MXene nanocomposite films in categories, and summarize the different strategies for fabricating high performance graphene and MXene nanocomposite films. Then, the applications of thermal management and electromagnetic interference (EMI) shielding have been discussed. Finally, we conclude the prospects and challenges about how to fabricate high performance nanocomposite films.

2 Preparation methods

Inspired by lamellar structure of nacre, many methods have been developed for preparing graphene and MXene nanocomposite films, containing vacuum-assisted filtration (VAF) [23,31–36], blade coating [37,38], drop casting [19,39] and layer-by-layer (LbL) [40,41]. VAF is a facile preparation method with convenient operation for assembling 2D nanosheets into nanocomposite films (Fig. 1a). The free-standing graphene film on the substrate can be formed with graphene nanosheets stacking with each other under a directional flow. And the film thickness is ranging through controlling the volume of dispersion. Dikin et al. [17] reported the strong free-standing GO films by VAF for

the first time in 2007. After that, various kinds of graphene nanocomposite films have been reported. On the other hand, the MXene nanosheets have been also assembled into free-standing MXene films by VAF in 2013 [12]. However, the longtime fabrication process and small size of obtained film are limited the practical application. In order to fabricate large area nanocomposite films, various preparing methods, such as blade coating and drop casting, have been used to effectively prepare the nanocomposite films. Blade coating is generally applied in scalable and continuous production of nanocomposite films. Normally, the large area nanocomposite films are prepared by scraping and moving slurry with blade on the substrate. And the thickness of obtained nanocomposite film is controlled by the blade height and speed. For instance, Zhang et al. [42] prepared GO films by blade coating method. After graphitization and hot-pressing, the resultant 200-μm-thick graphene films show ultrahigh thermal conductivity of 1224 W/mK. Moreover, Li et al. [38] fabricated the MXene/Polyvinylidene fluoride (PVDF) nanocomposite films through blade coating process with high shear force (Fig. 1b). However, this method is restricted to the concentration and viscosity of the material slurry. Moreover, drop casting is also widely applied in fabricating large-scale nanocomposite films. The nanocomposite films are prepared by casting dispersion onto the substrate followed by evaporation of solvent. For example, Shen et al. [19] prepared large-area GO film using drop casting of GO dispersion under heating, and the high thermal conductivity graphene EMI shielding film was obtained after graphitization treatment (Fig. 1c). Moreover, Zhong et al. [43] reported the free-standing MXene film via a drop casting method, which enhances the adhesion to the sulfur layer. However, the existing aggregation of nanosheets during the evaporation process may lead to the low performance. Except the above methods, the LbL assembly strategy is another method for preparing nanocomposite films, especially for 2D materials. Generally, the LbL assembly is a cyclical preparation process of fabricating multilayer structures by alternately depositing two different materials onto the substrate [44]. For example, Song et al. [41] prepared silicone rubber/graphene nanocomposite films with highly ordered multilayered structure by spinLbL, and the thermal conductivity of obtained nanocomposite films is 2.03 W/mK (Fig. 1d). However, the LbL assembly process is also time consuming and similar to the VAF method. Furthermore, the above preparation methods have been summarized and compared in the Table 1.

3 Mechanical properties
3.1 Graphene nanocomposite films
In the past several years, there are numerous efforts for fabricating the ultrastrong graphene nanocomposite films [45–47]. The main factors for fabricating high performance graphene nanocomposite films are strengthening interface interactions, enhancing alignment degree and reducing the voids. Generally, the interface interaction is a vital factor to enhance the mechanical properties of graphene nanocomposite films. The previous researches have demonstrated that the synergistic interface interactions are an effective strategy for fabricating high performance graphene nanocomposite films [48–50].
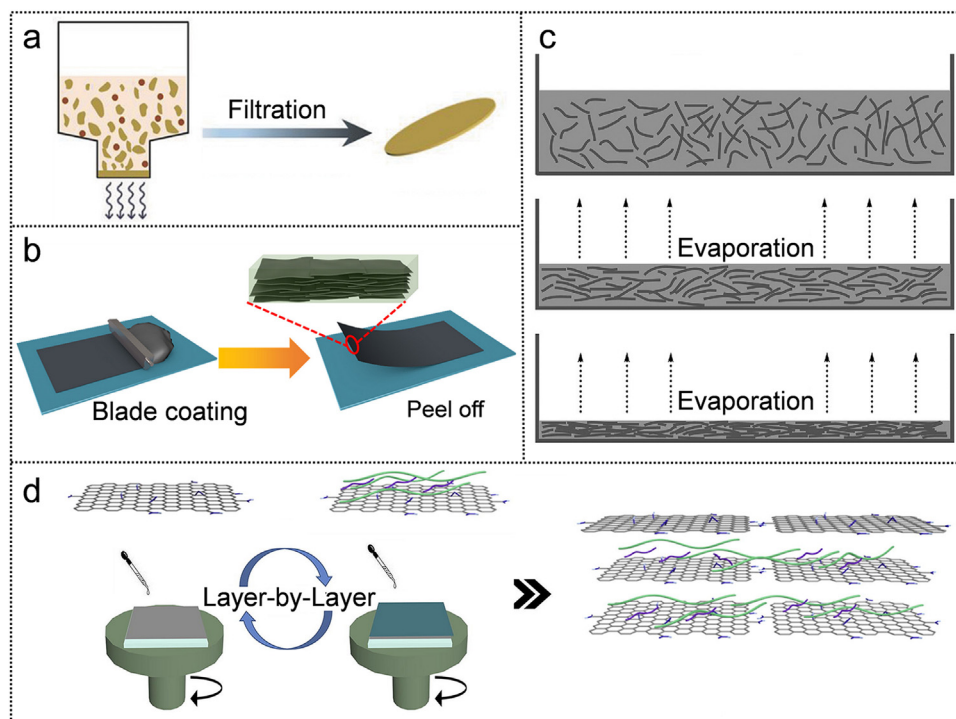
Fig. 1

Preparation methods of graphene and MXene nanocomposite films. (a) Schematic diagram of the vacuum-assisted filtration method for preparing graphene nanocomposite films. Reproduced with permission from Ref. [34] Copyright 2018, John Wiley and Sons. (b) Schematic diagram of the MXene/PVDF nanocomposite films by blade coating method. Reproduced with permission from Ref. [38] Copyright 2021, Elsevier. (c) Schematic diagram of the large-area graphene film through drop casting method. Reproduced with permission from Ref. [19] Copyright 2014, John Wiley and Sons. (d) Schematic diagram of the Layer-by-Layer method for preparing silicone rubber/graphene nanocomposite films. Reproduced with permission from Ref. [41] Copyright 2018, Elsevier.

Table 1

Comparison of preparing methods for fabricating graphene and MXene nanocomposite films.

Preparing methods	Advantages	Disadvantages	Film size
Vacuum-assisted filtration	Facile, controllable thickness	Time-consuming	Centimeter level
Blade coating	Continuous, scalable, quick	Raw material-consuming	Meter-level
Drop casting	Scalable, quick	Easy aggregation	Meter-level
Layer-by-layer	Easy and precise control structure	Time-consuming	Centimeter level

For instance, Xiong et al. [51] prepared the ultrarobust and transparent reduced graphene oxide (rGO)/cellulose nanocrystal (CNC) nanocomposite films via LbL method through hydrogen bonding and ionic interactions, which has greatly improved the interfacial interactions. Consequently, the obtained rGO/CNC nanocomposite film shows a high tensile strength of 655 MPa and a Young's modulus of 169 GPa, respectively. Moreover, Cheng et.al [52] demonstrated the rGO/chitosan (CS)/Cu^{2+} nanocomposite films with an improved synergistic effect of metal-ligand coordinate bonding through copper ions (Fig. 2a). The resultant rGO/CS/Cu^{2+} nanocomposite film shows high tensile strength of 868.8 MPa and electrical conductivity of 23480 S/m, respectively (Fig. 2b). Meanwhile, the novel sequential bridging strategy of ionic bonding and π-π interaction for preparing strong and highly conductive graphene nanocomposite films is demonstrated by Wan et al [4] (Fig. 2c). First, the GO nanosheets are bridged with

chromic ion through ionic bonding, and then the 1-pyrenebutyric acid N-hydroxysuccinimide ester-1-aminopyrene (PSE-AP) is introduced into the ionically bridged rGO hybrid to fabricate the sequentially bridged rGO (SBG) nanocomposite films. And the tensile strength, toughness and electrical conductivity of SBG nanocomposite film are 821 MPa, 20 MJ/m^3 and 41600 S/m, respectively, demonstrating 4.0, 7.5 and 1.9 folds higher than that of rGO film. Moreover, the SBG nanocomposite film also exhibits the excellent stability in harsh environments.

The other kind of synergistic effect from ionic bonding and covalent interaction also result in high performance graphene nanocomposite films. For instance, Wan et al. [46] introduced the nickel ion and poly(dopamine) (PDA) into GO nanosheets to form chelate architecture. The resultant graphene nanocomposite film shows a tensile strength of 417.2 MPa and toughness of 19.5 MJ/m^3, respectively. Furthermore, the strong covalent interaction
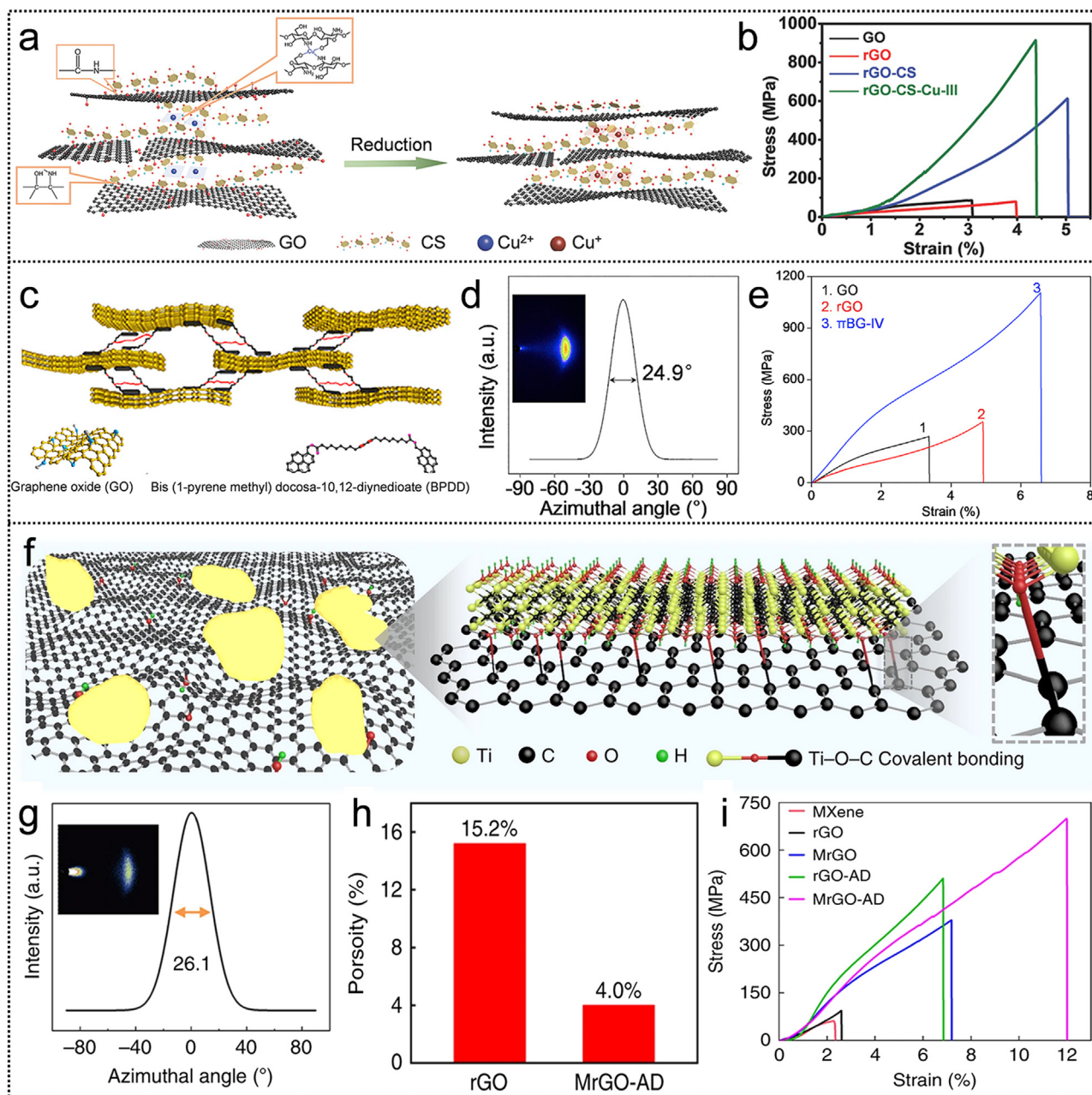
Fig. 2

Mechanical properties of graphene nanocomposite films via synergistic interface interactions. (a) Schematic diagram of rGO/CS/Cu^{2+} nanocomposite films. (b) Stress-strain diagrams of pristine GO, rGO, rGO/CS and rGO/CS/Cu^{2+} nanocomposite films. Reproduced with permission from Ref. [52] Copyright 2018, John Wiley and Sons. (c) Schematic diagram of πBG nanocomposite films. (d) The Wide-angle X-ray scattering patterns of πBG nanocomposite films. (e) Stress-strain diagrams of GO, rGO and πBG nanocomposite films. Reproduced with permission from Ref. [23] Copyright 2019, Elsevier. (f) Schematic diagram of MrGO-AD nanocomposite films. (g) The Wide-angle X-ray scattering patterns of MrGO-AD nanocomposite films. (h) The porosity of rGO and MrGO-AD nanocomposite films. (i) Stress-strain diagrams of MXene, GO, rGO-AD, MrGO and MrGO-AD nanocomposite films. Reproduced with permission from Ref. [36] Copyright 2020, Springer Nature.

and weak hydrogen bonding also can be integrated to achieve synergistic effect. Wan et al. [45] reported the strong and tough graphene nanocomposite films through synergistic interactions of hydrogen bonding and covalent interaction via a simple VAF method. When the content of CS is 5.6 wt%, the graphene nanocomposite film shows a tensile strength of 526.7 MPa, toughness of 17.7 MJ/m^3, indicating 4 and 10 times higher than natural nacre, respectively. Moreover, some other synergistic

effects, such as hydrogen bonding and π–π interaction [53], have been investigated to heighten the mechanical properties of graphene nanocomposite films.

Besides strong interfacial interactions, alignment and compactness of 2D nanosheets in nanocomposite films are extremely vital for optimizing the mechanical properties. Recently, Wan et al. [23] proposed a novel strategy that the long-chain π-bonding can markedly increase the alignment

degree of graphene nanosheets. The rGO films are immersed into the solution of highly π-conjugated long-chain polymer of bis(1-pyrenemethyl) docosa-10,12-diynedioate (BPDD), followed by UV irradiation, resulting in ultrastrong π-bridged rGO (πBG) nanocomposite films. Moreover, the πBG nanocomposite film shows a narrower full width at half maximum (FWHM) (24.9°) than the pure rGO film (35.5°), indicating the higher alignment of πBG nanocomposite film (Fig. 2d). Hence, the resultant πBG nanocomposite film exhibits an ultrahigh strength of 1054 MPa and toughness of 36 MJ/m^3, demonstrating 2.9 and 4.6 folds higher than pristine rGO film, respectively (Fig. 2e). Moreover, the electrical conductivity of πBG nanocomposite film reaches up to 119,200 S/m.

Furthermore, filling small size nanosheets is another effective strategy for constructing the high performance nanocomposite films. For instance, Zhou et al. [36] demonstrated the outstanding mechanical and electrical conductivity properties MXene-functionalized graphene (MrGO-AD) nanocomposites using small size nanosheets filling strategy (Fig. 2f). The small size MXene nanosheets are introduced to covalently crosslinked graphene nanosheets, which also are crosslinked by 1-aminopyrene-disuccinimidyl suberate (AD) molecules through π–π interaction. Then, the voids in nanocomposites are dramatically reduced from 15.2% for pure rGO film into 4.0 % for MrGO-AD nanocomposite film. Meanwhile, the alignment degree of graphene nanosheets are also improved for MrGO-AD film with a narrower FWHM of 26.1° compared to the pure rGO film with FWHM of 36.3° (Fig. 2g and h). Then, the MrGO-AD nanocomposite film shows an improved tensile strength of 699.1 MPa, ultrahigh toughness of 42.7 MJ/m^3 and electrical conductivity of 132,900 S/m, respectively (Fig. 2i). Besides the Mxene nanosheets, some other nanosheets such as montmorillonite (MMT) [33], Tungsten disulfide (WS$_2$) [47], Molybdenum sulfide (MoS$_2$) [54] and black phosphorus (BP) [31] etc. are also utilized to construct the ultrastrong graphene nanocomposite films in the past few years.

In addition, the external force induced orientation strategies such as blade coating [40], plasticization stretching [55], scanning centrifugal casting [56] and freezing stretching strategies [57], are developed to improve the alignment degree of nanosheets and reduce existing voids of nanocomposite films. For instance, Akbari et al. [58] demonstrated the highly ordered and compactness graphene films by shear alignment through blade coating method. First, the small size rGO nanosheets are introduced into the GO precursor. After rolling press and high temperature treatment, the highly dense graphitic films are obtained. This method results in higher alignment of in-plane direction due to the lower FWHM of the Raman G band. The tensile strength of highly dense graphitic film reaches up to 78.5 MPa when the rGO content of 15 wt%. Moreover, Zhang et al. [59] demonstrated a novel chemical-structure-engineering strategy for gaining involuntarily regular stacking of GO nanosheets during the liquid-assembly process to fabricate the highly aligned microstructure GO films. And the obtained GO film shows a high strength of 445 MPa and a Young's modulus of 52.3 GPa, respectively. Furthermore, Li et al. [55] prepared the macroscopic graphene nanocomposite film via a continuous plasticization stretch method, eliminating the wrinkling of graphene nanosheets into crystalline orders (Fig. 3a).

During the plastic transition process, the direct-cast GO film is immersed into ethanol leading to a transition from a brittle to a plastic state due to the intercalation of solvent molecules. And the wrinkling of GO film is eliminated during the stretching process resulting in a high Herman's order parameter of 0.93. This method endows the graphene films excellent mechanical properties with the tensile strength of 1.1 GPa and Young's modulus of 62.8 GPa (Fig. 3b). Besides, Wei et al. [56] demonstrated a high alignment pristine graphene nanocomposite film with outstanding EMI shielding performance and mechanical properties through a scanning centrifugal casting method. And the obtained 100-μm-thick graphene nanocomposite film exhibits the ultrahigh EMI SE of 93 dB and a high tensile strength of 145 MPa.

Recently, Cheng's group demonstrated a record-breaking graphene nanocomposite film via freezing stretch-induced alignment of graphene nanosheets with interfacial interactions [57]. First, the GO nanocomposite film is prepared via a simple VAF method (Fig. 3c). Then, the GO nanocomposite film is biaxially stretched and infiltrated into the polymerization of 10,12-pentacosadiyn-1-ol (PCO, (CH$_3$(CH$_2$)$_{11}$C≡C-C≡C(CH$_2$)$_8$CH$_2$OH) solution to form a BS-GO-PCO nanocomposite films. Next, after HI reduction, the BS-rGO-PCO nanocomposite film is immersed into the PSE abd AP solution to form π-π interaction and fabricate the SB-BS-rGO nanocomposite film. The SB-BS-rGO nanocomposite films have highly compact graphene nanosheets stacking and fewer voids than pristine rGO films. And the porosity of SB-BS-rGO nanocomposite film shows only 9.30%, which is lower than the pristine rGO film of 18.7%. Moreover, the SB-BS-rGO nanocomposite film exhibits an ultrahigh Herman's orientation factor of 0.956, which is higher than the pristine rGO film. The SB-BS-rGO nanocomposite film shows a record tensile strength of 1547 MPa, which is higher than the previous reports. Moreover, the toughness and Young's modulus of SB-BS-rGO nanocomposite film reach up to 35.9 MJ/m^3 and 64.5 GPa, respectively. The developed freezing stretch-induced alignment provides a promising strategy for preparing high performance graphene nanocomposite films, which can also be used to other 2D materials such as MXene.

3.2 MXene nanocomposite films

The outstanding mechanical property of MXene nanocomposite films is an important prerequisite for using in many application fields [18,60-64]. Compared with graphene, the MXene has abundant surface functional groups (-F, -O and -OH) without any chemical modification, which is easy for constructing interfacial interactions between MXene nanosheets via hydrogen, ionic and covalent bonding. For instance, Ling et al. [18] introduced the polyvinyl alcohol (PVA) into the MXene to prepare the strong and free-standing composite films for the first time in 2014. The tensile strength of MXene/PVA nanocomposite films is 91 MPa when adding 60 wt% PVA, which is higher than pure MXene film with tensile strength of 22 MPa. However, high content of PVA in the nanocomposite film endows the poor electrical conductivity of 0.04 S/m. Moreover, Cao et al. [21] reported the strong and tough MXene/cellulose nanofiber (CNF) nanocomposite films through a facile VAF method (Fig. 4a). The CNF shows excellent mechanical properties such as strength
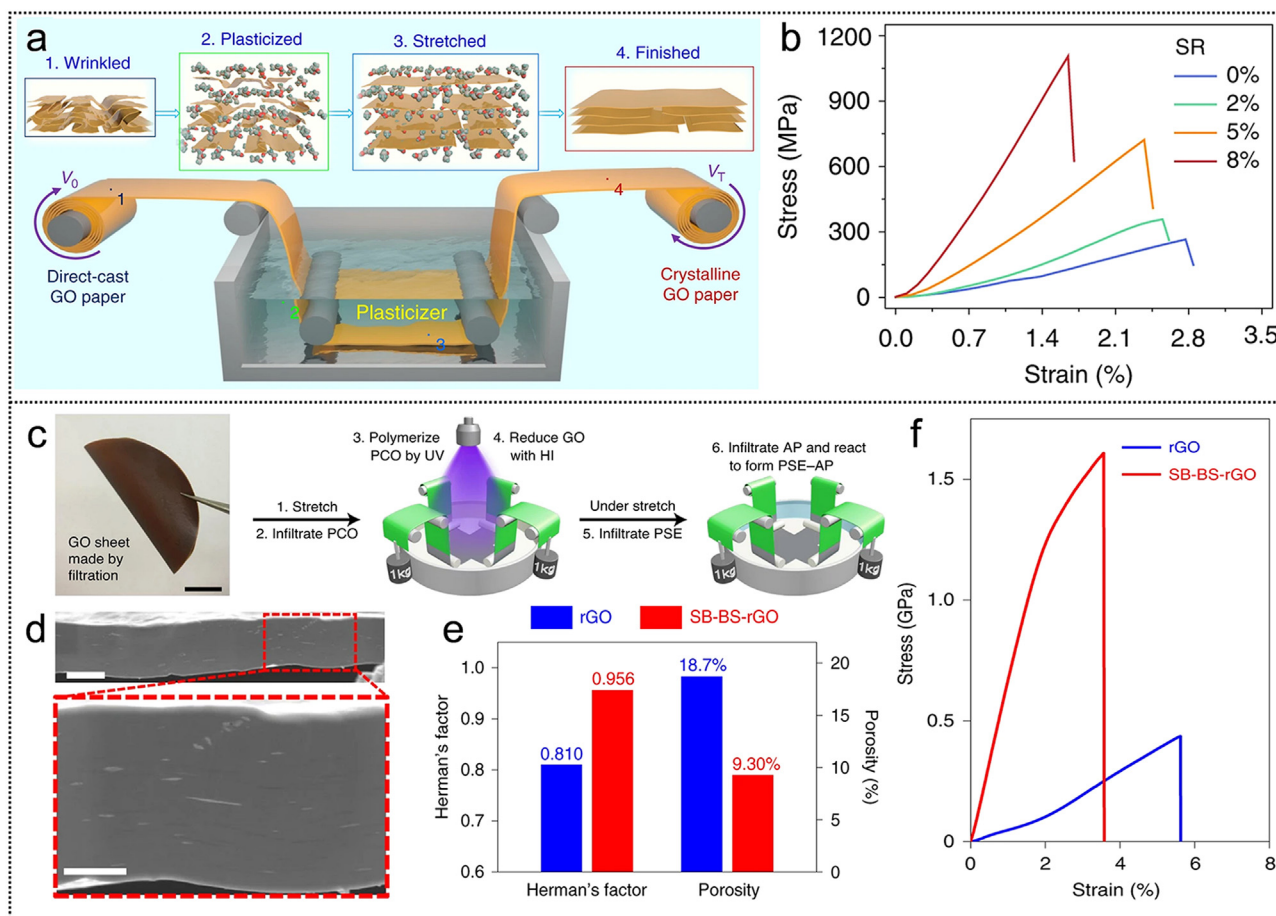
Fig. 3

Mechanical properties of graphene nanocomposite films via external force induced orientation. (a) Schematic diagram of graphene films through plasticization stretching method. (b) Stress-strain curves of graphene films. (c) Schematic diagram of BS-SB-rGO nanocomposite films. Reproduced with permission from Ref. [55] Copyright 2020, Springer Nature. (d) Cross-sectional SEM images cut by FIB for SB-BS-rGO nanocomposite film. (e) Porosity and Herman's orientation factor of pure rGO and BS-SB-rGO nanocomposite films. (f) Stress-strain diagrams of rGO and SB-BS-rGO nanocomposite films. Reproduced with permission from Ref. [57] Copyright 2021, Springer Nature.

and flexible with unique1D nanofiber structure and abundant surface groups, and can easily form hydrogen bonding with MXene nanosheets. Moreover, MXene/CNF nanocomposite film displays a highly aligned layered structure, which is similar to the "brick-and-mortar" structure of nacre. The MXene/CNF nanocomposite film exhibits a high tensile strength of 135.4 MPa and toughness of 14.8 MJ/m^3, Young's modulus of 3.8 GPa via adding 50 wt% MXene (Fig. 4b). The nanocomposite film can be folded after 14260 times under a 4.9 N pulling load, indicating excellent durability for practical application. Except the PVA and CNF, various filler materials such as sodium alginate (SA) [35], poly(3,4-ethylenedioxythiophene)−poly-(styrenesulfonate) (PEDOT:PSS) [65], carboxymethyl cellulose (CMC) and aramid nanofiber (ANF) [18] are also introduced into the MXene to enhance the mechanical properties through hydrogen bonding. Furthermore, Liu et al. [66] demonstrated high performance MXene nanocomposite films by improving the interfacial interaction between the MXene nanosheets and multivalent aluminum ions (Al) via a VAF method. The tensile strength and Young's modulus of resultant MXene/Al nanocomposite

film are 83.2 MPa and 7.42 GPa, indicating 2.9 and 3.6 folds higher compared to MXene film respectively. Moreover, the MXene/Al nanocomposite film shows a high electrical conductivity of 265,600 S/m. However, the improvement in mechanical properties still need much more interface interactions in MXene nanocomposite films, especially for synergistic effect.

For instance, Lee et al. [67] demonstrated a spontaneous in situ polymerization of polydopamine with MXene (Fig. 4c) to obtain polydopamine-treated MXene nanocomposite films. The coordination and hydrogen bondings between MXene nanosheets are achieved during polymerization, improving the highly alignment and compactness of MXene nanosheets and eliminating the voids in the resultant nanocomposite films. The tensile strength reaches up to 309.8 MPa, which is 6.99 folds higher compared to pure MXene film (Fig. 4d). Meanwhile, the toughness and Young's modulus also reach up high value to 4.38 MJ/m^3 and 17.5 GPa, respectively. Moreover, the resultant nanocomposite film also shows a high electrical conductivity of 514,100 S/m. Furthermore, Zhang et al. [37] demonstrated highly ordered and compactness MXene films by using large size
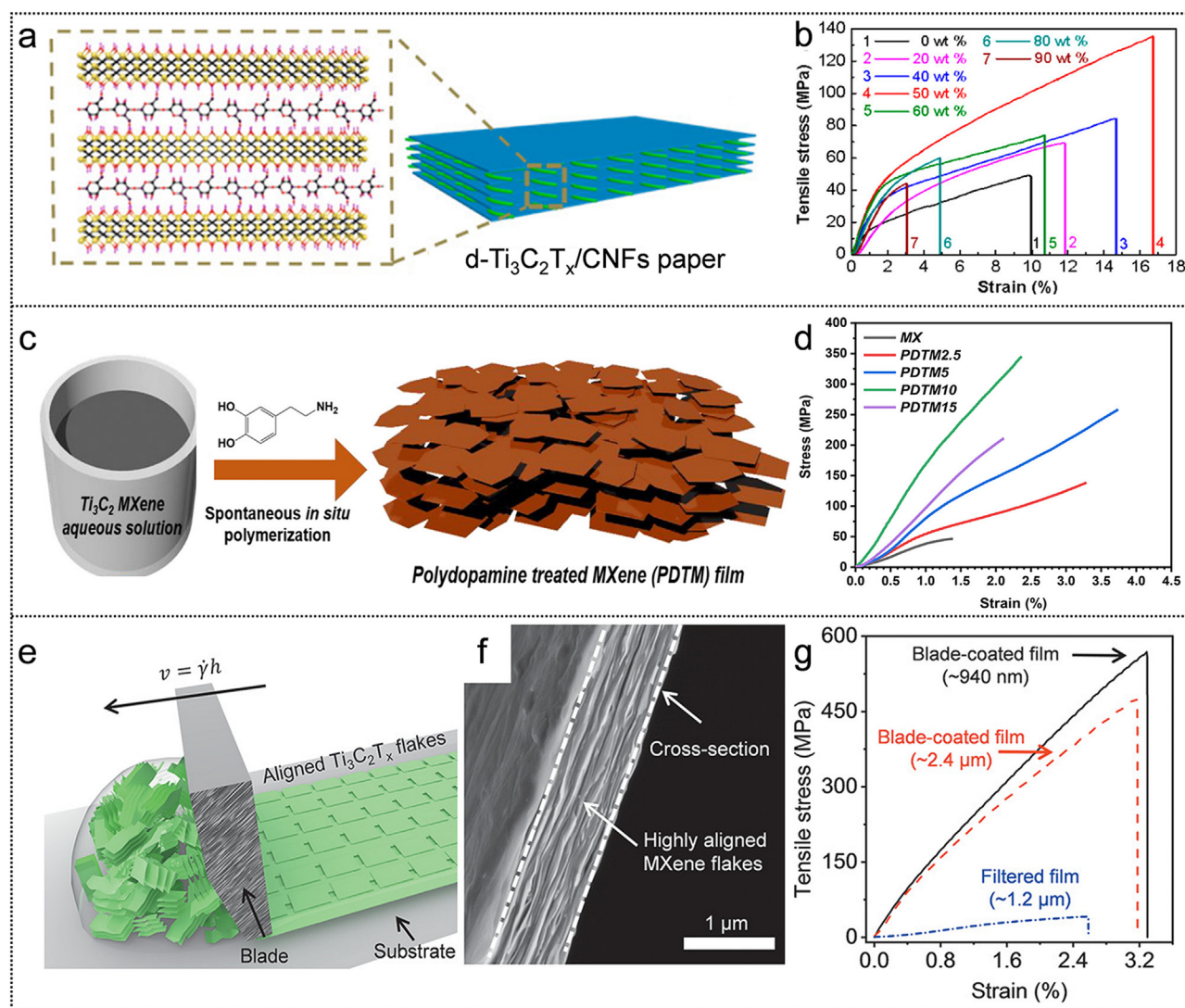
Fig. 4

Mechanical properties of MXene nanocomposite films via interface interactions and external force induced orientation. (a) Schematic diagram of MXene/CNF nanocomposite films. (b) Stress-strain diagrams of MXene/CNF nanocomposite films. Reproduced with permission from Ref. [21] Copyright 2018, American Chemical Society. (c) Schematic diagram of polydopamine-treated MXene nanocomposite films. (d) Stress-strain diagrams of polydopamine-treated MXene nanocomposite films. Reproduced with permission from Ref. [67] Copyright 2020, American Chemical Society. (e) Schematic diagram of MXene films through blade coating method. (f) Cross-sectional SEM images of MXene films. (g) Stress-strain diagrams of blade-coated MXene films. Reproduced with permission from Ref. [37] Copyright 2020, John Wiley and Sons.

MXene nanosheets via a blade coating method (Fig. 4e and 4f). By optimizing the shear force, blade speed and concentration, the MXene film exhibits excellent mechanical properties. The MXene film shows a ultrahigh tensile strength of 436 MPa, toughness of 10.2 MJ/m^3 and Young's modulus of 20.6 GPa, respectively (Fig. 4g). Moreover, the mechanical properties of MXene films composed of large size MXene nanosheets are better than those composed of small size MXene nanosheets. Meanwhile, the resultant MXene film shows a record electrical conductivity of 151,0000 S/m after heat treatment.

In addition, Cheng's group demonstrated the sequential bridging strategy for fabricating high performance MXene nanocomposite films through assembling MXene nanosheets. For instance, Wan et al. [60] fabricated the high performance MXene nanocomposite films through a sequential bridging of hydrogen and ionic bonding. The SA molecule is introduced into the MXene nanosheets to form hydrogen bonding, after that, the calcium ion (Ca^{2+}) is infiltrated into the MXene/SA nanocomposite films to achieve the sequentially bridged MXene (SBM) nanocomposite films through ionic bonding. The SBM nanocomposite film shows a high tensile strength of 436 MPa, Young's modulus of 14 GPa and toughness of 8.39 MJ/m^3, respectively, indicating 6.9, 2.5 and 13.5 folds higher compared to pure MXene films. Moreover, the electrical conductivity of SBM nanocomposite films is reached up to 298,800 S/m.

Very Recently, Cheng's group found that the existing voids in MXene nanocomposite films have a strong impact on the mechanical and electrical properties. Hence, Cheng's group
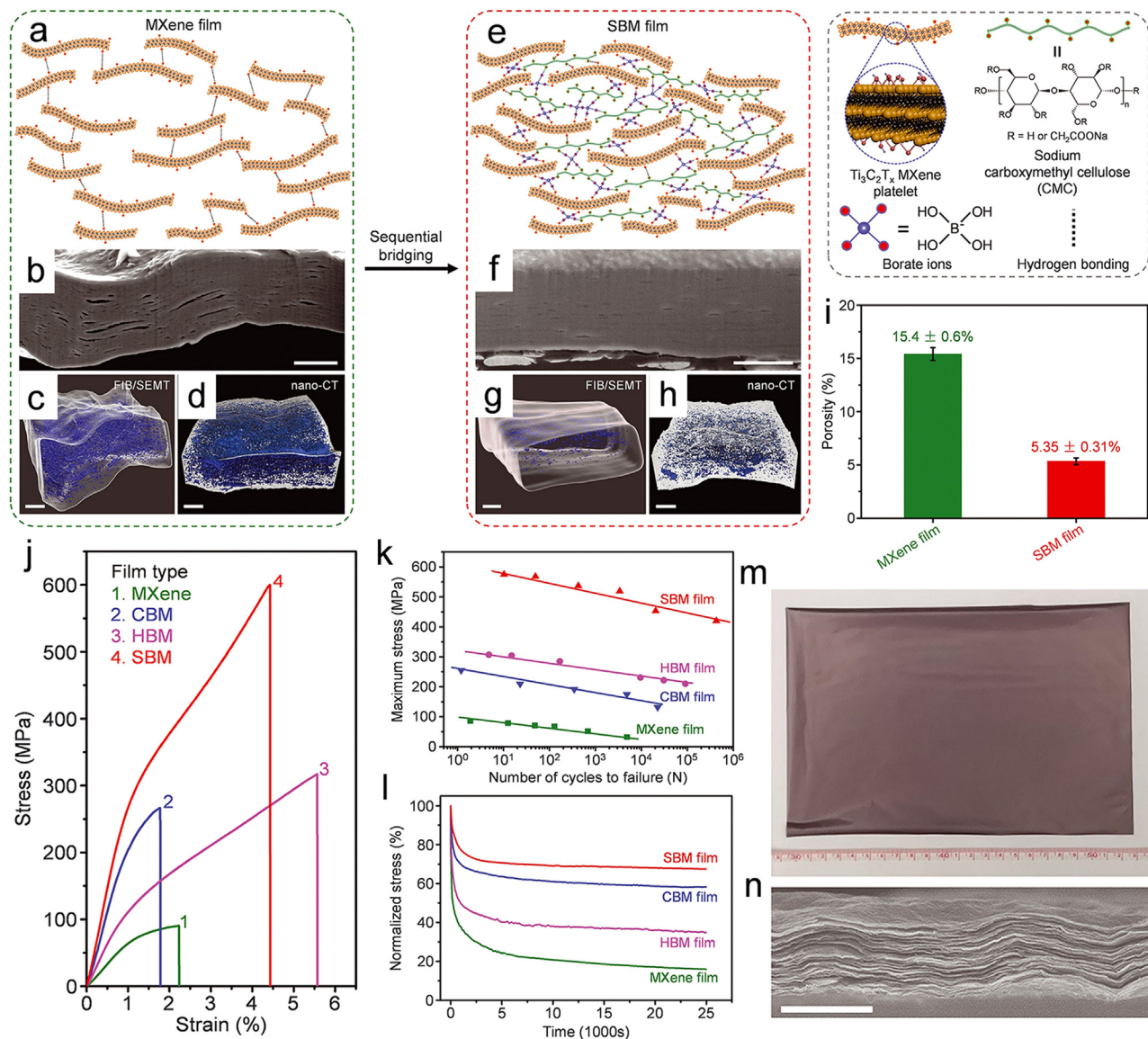
Fig. 5

Sequential bridging high strength MXene nanocomposite films. (a and e) Model structure representation of pure MXene film and SBM nanocomposite film. (b and f) Cross-sectional SEM images cut by FIB for pure MXene film and SBM nanocomposite film. (c and g) Three dimensional remodeled void microstructure root in FIB/SEMT for pure MXene film and SBM nanocomposite film. (d and h) Three dimensional remodeled void microstructure root in nano-CT for pure MXene film and SBM nanocomposite film. (i) Porosities of pure MXene film and SBM nanocomposite film root in density measurements. (j) Representative stress–strain diagrams of pure MXene film, covalent bonding MXene (CBM), hydrogen bonding MXene (HBM), and SBM nanocomposites. (k) Variations of maximum applied stress of MXene, CBM, HBM and SBM films after manifold cycles fatigue test. (l) Relationship between the time and the normalized stress level for MXene, CBM, HBM and SBM nanocomposite films. (m) The photograph of large area SBM nanocomposite films prepared by blade coating. (n) Cross sectional SEM image of large area SBM nanocomposite films. Reproduced with permission from Ref. [22] Copyright 2021, AAAS.

developed an effective densification strategy to remove voids through sequential bridging of hydrogen bonding and covalent interaction [22] (Fig. 5a and e). First, the CMC molecular is introduced into the MXene nanosheets to fabricate the hydrogen bonded MXene (HBM) nanocomposite films. Then, the boron ions are infiltrated into the HBM nanocomposite films to form ionic bonding and fabricate the sequentially bridged MXene (SBM) nanocomposite films. Moreover, the voids microstructure of pure MXene and SBM nanocomposite films have been remodeled by FIB and SEM tomography and nanoscale x-ray

computed tomography (Fig. 5b-h). The SBM nanocomposite films exhibit highly alignment, compactness structure and fewer voids compared to pure MXene films. And the porosity of SBM nanocomposite films is reduced to 5.35% from 15.4% for pure MXene film (Fig. 5i). Due to the improving microstructure of SBM nanocomposite films, the mechanical properties also have been enhanced. The SBM nanocomposite film exhibits a record tensile strength of 583 MPa, Young's modulus of 27.8 GPa and toughness of 15.9 MJ/m^3, respectively, which are 5.7, 11.2 and 3.6 folds higher compared to pure MXene film (Fig. 5j).

Furthermore, the SBM nanocomposite show outstanding fatigue resistance and remain 69.5% maximum stress after 420000 cycles stretching (Fig. 5k). Meanwhile, the SBM nanocomposite film shows higher relaxation resistance and can remain 67.5% of original stress after 25000 s relaxation (Fig. 5l). The large area SBM nanocomposite films also can be fabricated via blade coating method. Furthermore, the lateral size of SBM nanocomposite film is 23×14 cm^2 (Fig. 5m and n). And the SBM nanocomposite films (blade coating) also display a high tensile strength of 559 MPa, which is closed to the SBM nanocomposite film prepared by VAF method.

4 Applications

4.1 Thermal conductivity

The outstanding thermal conductivity of materials is vital to enhance heat diffusion and preserve electrical devices especially in the aerospace field. Single layer graphene nanosheet exhibit the ultrahigh thermal conductivity of over 5000 W/mK, indicating the potential application for thermal management field [8]. However, graphene nanocomposite films have not realized such high inherent thermal conductivity because of the existing voids and defects during the assembling of graphene nanosheets. Hence, the alignment and compactness of graphene nanocomposite films are required for high thermal conductivity. For instance, highly thermal conductive films composed of GO nanosheets and small rGO nanosheets are fabricated through blade coating followed by heat treatment rolling press and secondary heat treatment [58] (Fig. 6a). The obtained graphene films with high alignment and compactness structure show a high thermal conductivity of 2025 W/mK (Fig. 6b). Moreover, the plasticization stretching method can also increase the thermal conductivity. The thermal conductivity of graphene film under a stretching ratio of 8% is 109.1 W/mk, which is higher than that of no stretching graphene film of 42.34 W/mK [55]. Furthermore, Li et al. [68] proposed a novel strategy of camphor-assisted "cooling-contraction" for fabricating free-standing and high thermal conductivity graphene films with nanometer thickness. And the nanometer graphene film shows a ultrahigh thermal conductivity of 2820 W/mK with a thickness of 24 nm. However, up to now, most high thermal conductivity graphene films need ultrahigh temperature (over 2000 °C) or chemical reduction treatment, which is limited their practical application.

In recent years, MXene displays promising potential for fabricating high thermal conductivity films due to the intrinsic high thermal conductivity from theoretical simulation [69]. Moreover, compared with graphene, MXene has abundant surface functional groups, which can easily improve the interfacial interaction with other materials in nanocomposite films. However, the thermal conductivity of macroscopical MXene nanocomposite films is also inferior to its theoretical value. For instance, Li et al. [70] prepared high anisotropic thermal conductivity MXene/MMT nanocomposite films (Fig. 6c). The introduced MMT nanosheets can improve the alignment degree of MXene nanosheets in the nanocomposite films. The obtained nanocomposite film shows a high anisotropic thermal conductivity of 28.8 W/mK (in-plane) and 0.27 W/mK (cross-plane) (Fig. 6d). Moreover, Jin et al. [71] reported a MXene/PVA

multilayered nanocomposite film via multilayered drop casting method. The 27-μm-thick MXene/PVA nanocomposite film exhibits a high thermal conductivity of 4.57 W/mK, which is 23 folds higher compared to pure PVA film. Furthermore, several fillers such as CNF [72], AgNWs [72] and GO [73] are introduced into MXene to fabricate high thermal conductivity MXene nanocomposite films. Up to now, the thermal conductivity of MXene nanocomposite films is still at a low level. The existing voids and defects may be the main limiting factor for fabricating high thermal conductivity MXene nanocomposite films.

4.2 EMI shielding

With the rapid arrival of 5G era, the wireless gigahertz electromagnetic wave technique has been widely applied in human society. Meanwhile, the EMI pollution has been aroused more consideration. Graphene is considered as promising alternatives to traditional material of metal for fabricating outstanding EMI shielding materials due to the unique lamellar structure, high electrical conductivity and large aspect ratios [74]. For instance, Xi et al. [75] demonstrated the multilayered graphene aerogel films (GAF) using the HI reduction and high temperature treatment through the GO film. The 120-μm-thick GAF shows an exccellent EMI shielding performance of 105 dB due to the expansion enhancement effect. Moreover, Wan et al. [23] demonstrated the graphene nanocomposite films by long chain π bridging. And the obtaining π bridging graphene nanocomposite film shows an excellent EMI SE of 36.5 dB, which is higher than the pure rGO film of 24.9 dB. In addition, for eliminating the influence of thickness on EMI shielding performance, the absolute EMI SE effectiveness (SSE$_t$) of materials is defined as SE divided by the thickness and density. The π bridging graphene nanocomposite film shows a high SSE$_t$ of 53409 dB cm^2/g, which is higher compared to most reported EMI shielding materials. However, most graphene EMI shielding nanocomposite films are undergone the chemical or heat treatment reduction process, which is restricted the practical application and influenced the EMI shielding performance. Hence, Wei et al. [56] reported high alignment lamellar structure pure graphene films and graphene nanocomposite films via an efficient and scalable scanning centrifugal casting method (Fig. 6e). The 100-μm-thick pure graphene film shows a superhigh EMI SE of 93 dB (Fig. 6g). When the electromagnetic waves (EMWs) interact with the surface of a graphene nanosheet, some of incident EMWs are immediately reflected because of the high electrical conductivity of graphene nanosheets (Fig. 6f). Then, the other EMWs are partially absorbed through graphene layer, leading to the attenuation of EMWs. Moreover, the surviving EMWs pass through next MXene layer and repeat the attenuation. Meanwhile, the EMWs are reflected between the adjacent graphene layers until completely absorbed. Furthermore, the highly ordered lamellar structure provides more multiple interfacial reflections, resulting highly efficient EMI shielding performance.

Recently, MXene is known as the ideal candidate for fabricating high EMI shielding performance materials due to its outstanding conductivity and abundant surface groups [35,76-79]. For example, Yury's group [35] first reported several kinds of pure
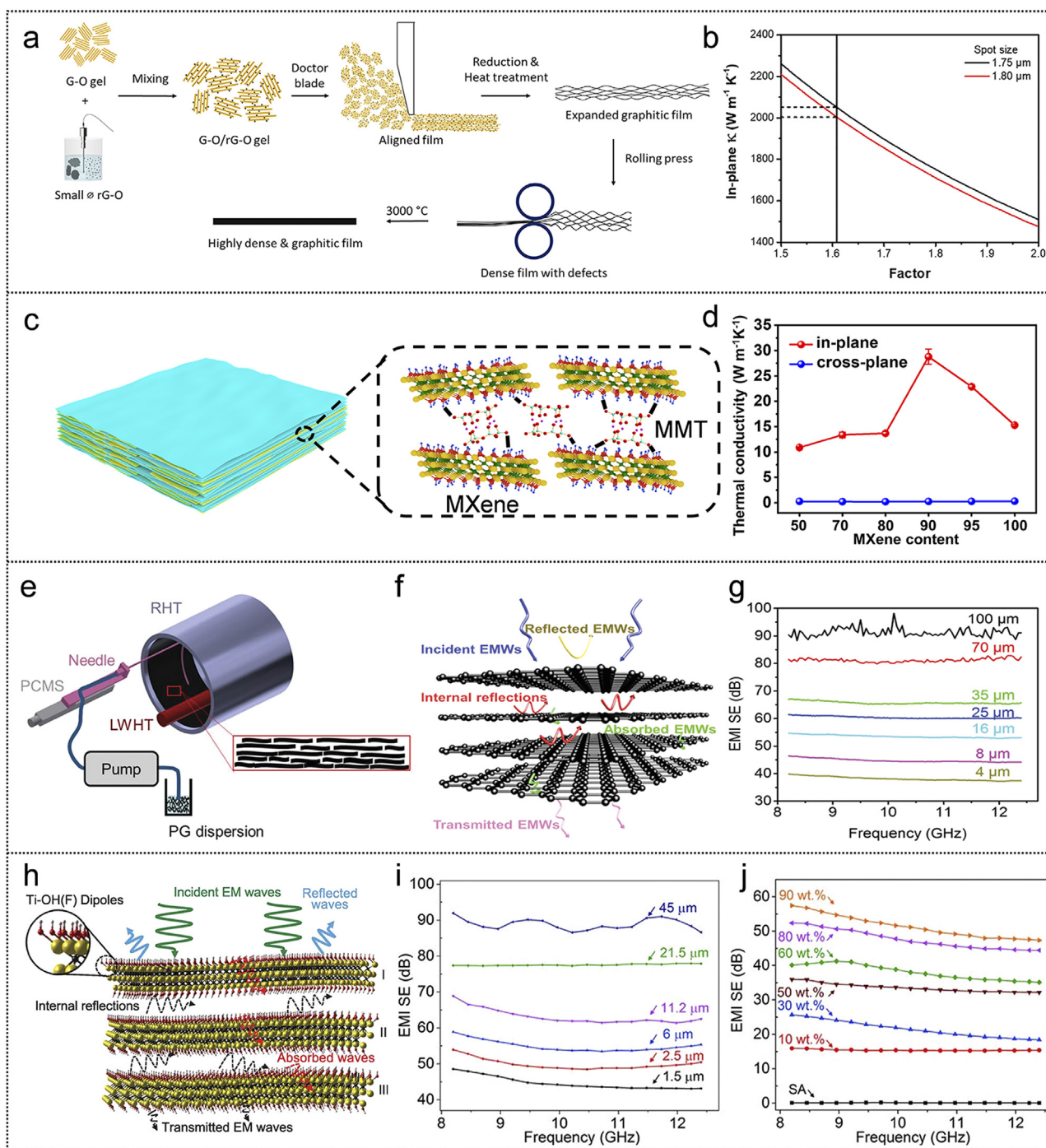
Fig. 6

Application of graphene and MXene nanocomposite films. (a) Schematic diagram of the fabrication process of graphene films. (b) Thermal conductivity of graphene nanocomposite films. Reproduced with permission from Ref. [58] Copyright 2020, Elsevier. (c) Schematic diagram of the MXene/MMT nanocomposite films. (d) Thermal conductivity of MXene/MMT nanocomposite films. Reproduced with permission from Ref. [70] Copyright 2020, American Chemical Society. (e) Schematic diagram of the fabrication process of pure graphene films through scanning centrifugal casting. (f) Schematic diagram of the EMI shielding mechanism of pure graphene films. (g) EMI SE of pure graphene films with different thickness. Reproduced with permission from Ref. [56] Copyright 2020, John Wiley and Sons. (h) Schematic diagram of the EMI shielding mechanism of pure MXene films. (i) EMI SE of $Ti_3C_2T_x$ MXene films with different thickness. (j) EMI SE of MXene/SA nanocomposite films with different MXene content. Reproduced with permission from Ref. [35] Copyright 2016, AAAS.

MXene and MXene nanocomposite films for EMI shielding via a simple VAF method (Fig. 6h). And the 45-μm-thick $Ti_3C_2T_x$ MXene film shows an ultrahigh EMI SE of 92 dB (Fig. 6i). Moreover, the natural biomaterials of SA are introduced into the MXene to form hydrogen bonding with the surface functional groups of MXene. The 8-μm-thick MXene/SA nanocomposite film shows an EMI SE of 57 dB via adding 10 wt% SA (Fig. 6j). Moreover, the SSE_t of pure MXene film and MXene/SA nanocomposite film are 25863 and 30830 dB cm^2/g, which is higher than the traditional metal of pure aluminum and copper foils. After that, different MXene nanocomposite films are fabricated for EMI shielding performance. For instance, Cao et al. [21] prepared MXene/CNF nanocomposite films with an EMI SE of 25.7 dB and a SSE_t of 2647 dB cm^2/g via adding 20 wt% CNF. Moreover, Jin et al. [70] fabricated the multilayered MXene/PVA nanocomposite film with an EMI SE of 44.4 dB and a SSE_t of 9343 dB cm^2/g via adding 19.5 wt% MXene, which is higher than most polymer nanocomposite films at the same filler content. Very recently, Wan et al. [22] proposed a sequential bridging MXene nanocomposite film through hydrogen and covalent bonding. And the 3-μm-thick SBM nanocomposite film exhibits a high EMI SE of 56.4 dB and a SSE_t of 62458 dB cm^2/g.

5 Summary and outlook

In the past several years, two dimensional materials such as graphene and MXene have been widely studied owing to the excellent physiochemical properties. In this review, we have focused on the preparation methods, assembling strategies and mechanical properties of graphene and MXene nanocomposite films. Moreover, we have also discussed the applications of obtained graphene and MXene nanocomposite films such as EMI shielding and thermal conductivity. Various methods such as VAF, blade coating, drop casting and LbL have been used to prepare high performance graphene and MXene nanocomposite films. However, as aforementioned, the existing voids and wrinkling are harmful for the mechanical properties of graphene and MXene nanocomposite films. Hence, several strategies for fabricating high performance graphene and MXene nanocomposite films are proposed.

Inspired by nacre, the interfacial interactions, alignment and compactness are three important factors for fabricating strong and tough nanocomposite films. The interfacial crosslinking strategies mainly include hydron bonding, ionic bonding, π-π interaction and covalent interaction. And the obtained graphene and MXene nanocomposite films show the moderate mechanical properties, which are lower than theoretical prediction. It was found that the synergistic interactions effectively enhance the alignment and compactness of graphene and MXene nanocomposite films. Moreover, filling is another effective strategy to compact graphene and MXene film by curing the existing voids. Furthermore, the external force induced orientation strategies including blade coating, plasticization stretching, scanning centrifugal casting and freezing stretching are utilized to improve the alignment and eliminate the wrinkling and voids of graphene nanocomposite film. Compared to graphene nanocomposite films, the aforementioned strategies for fabricating high performance MXene nanocomposite films are

rarely investigated up to now except for interfacial interactions. Hence, other strategies such as filling and external force inducing are needed to be further explored. Meanwhile, the size and structure of graphene and MXene nanosheets is needed to be investigated deeply for constructing high performance nanocomposite films.

Despite the great research progress of mechanical properties have been realized, the functional applications of graphene and MXene nanocomposite films are equally important. Due to their intrinsic thermal and electrical conductivity, the graphene and MXene nanocomposite films have enormous promising potential used in EMI shielding and thermal management materials. However, there are still existing challenges needed to be investigated. With respect to graphene nanocomposite films, most graphene shielding nanocomposite films are needed chemical and heat treatment reduction process to realize their superior performance, limiting the practical application. Moreover, MXene can fabricate the high performance nanocomposite films directly compared with graphene. However, the MXene nanocomposite films display poor environmental stability especially in humid and high temperature environment. And the mechanical properties of pure MXene films are relatively low. Furthermore, the practical thermal conductivity of graphene and MXene nanocomposite films are far below the theoretical prediction. Hence, how to construct high performance graphene and MXene nanocomposite films is still a challenge to solve in the future research.

Currently, the obtained graphene and MXene nanocomposite films are prepared in a small size. Hence, as for practical application, the large size of graphene and MXene nanocomposite films with excellent performance are urgently needed. Finally, we believe that these nanocomposite films are successfully prepared for real-life applications and come about the near future.

Declaration of Competing Interest

The authors declare no conflict of interest.

Acknowledgments

Supplementary materials

Supplementary material associated with this article can be found, in the online version, at doi:10.1016/j.giant.2022.100117.

References

[1] K.S. Novoselov, A.K. Geim, S.V. Morozov, D. Jiang, Y. Zhang, S.V. Dubonos, I.V. Grigorieva, A.A. Firsov, Electric field effect in atomically thin carbon films, Science 306 (2004) 666–669, doi:10.1126/science.1102896.

[2] V. Nicolosi, M. Chhowalla, M.G. Kanatzidis, M.S. Strano, J.N. Coleman, Liquid exfoliation of layered materials, Science 340 (2013) 1226419, doi:10.1126/science.1226419.

[3] M.J. Allen, V.C. Tung, R.B. Kaner, Honeycomb carbon: a review of graphene, Chem. Rev. 110 (2010) 132–145, doi:10.1021/cr900070d.

Review

[4] A.K. Geim, K.S. Novoselov, The rise of graphene, Nat. Mater. 6 (2007) 183–191, doi:10.1038/nmat1849.

[5] K.S. Kim, Y. Zhao, H. Jang, S.Y. Lee, J.M. Kim, K.S. Kim, J.-H. Ahn, P. Kim, J.-Y. Choi, B.H. Hong, Large-scale pattern growth of graphene films for stretchable transparent electrodes, Nature 457 (2009) 706–710, doi:10.1038/nature07719.

[6] L. Lin, H. Peng, Z. Liu, Synthesis challenges for graphene industry, Nat. Mater. 18 (2019) 520–524, doi:10.1038/s41563-019-0341-4.

[7] C. Lee, X. Wei, J.W. Kysar, J. Hone, Measurement of the elastic properties and intrinsic strength of monolayer graphene, Science 321 (2008) 385–388, doi:10.1126/science.1157996.

[8] A.A. Balandin, S. Ghosh, W. Bao, I. Calizo, D. Teweldebrhan, F. Miao, C.N. Lau, Superior thermal conductivity of single-layer graphene, Nano lett 8 (2008) 902–907, doi:10.1021/nl0731872.

[9] X. Huang, X. Qi, F. Boey, H. Zhang, Graphene-based composites, Chem. Soc. Rev. 41 (2012) 666–686, doi:10.1039/c1cs15078b.

[10] Y.-Q. Li, T. Yu, T.-Y. Yang, L.-X. Zheng, K. Liao, Bio-inspired nacre-like composite films based on graphene with superior mechanical, electrical, and Biocompatible Properties, Adv. Mater. 24 (2012) 3426–3431, doi:10.1002/adma.201200452.

[11] A. VahidMohammadi, J. Rosen, Y. Gogotsi, The world of two-dimensional carbides and nitrides (MXenes), Science 372 (2021) eabf1581, doi:10.1126/science.abf1581.

[12] M.R. Lukatskaya, O. Mashtalir, C.E. Ren, Y. Dall'Agnese, P. Rozier, P.L. Taberna, M. Naguib, P. Simon, M.W. Barsoum, Y. Gogotsi, Cation intercalation and high volumetric capacitance of two-dimensional titanium carbide, Science 341 (2013) 1502–1505, doi:10.1126/science.1241488.

[13] M. Ghidiu, M.R. Lukatskaya, M.Q. Zhao, Y. Gogotsi, M.W. Barsoum, Conductive two-dimensional titanium carbide 'clay' with high volumetric capacitance, Nature 516 (2014) 78–81, doi:10.1038/nature13970.

[14] M. Naguib, M. Kurtoglu, V. Presser, J. Lu, J. Niu, M. Heon, L. Hultman, Y. Gogotsi, M.W. Barsoum, Two-dimensional nanocrystals produced by exfoliation of Ti_3AlC_2, Adv. Mater. 23 (2011) 4248–4253, doi:10.1002/adma.201102306.

[15] L. Li, M. Shi, X. Liu, X. Jin, Y. Cao, Y. Yang, W. Wang, J. Wang, Ultrathin Titanium carbide (MXene) films for high-temperature thermal camouflage, Adv. Funct. Mater. 31 (2021) 2101381, doi:10.1002/adfm.202101381.

[16] M. Shi, M. Shen, X. Guo, X. Jin, Y. Cao, Y. Yang, W. Wang, J. Wang, $Ti_3C_2T_x$ MXene-decorated nanoporous polyethylene textile for passive and active personal precision heating, ACS Nano 15 (2021) 11396–11405, doi:10.1021/acsnano.1c00903.

[17] D.A. Dikin, S. Stankovich, E.J. Zimney, R.D. Piner, G.H.B. Dommett, G. Evmenenko, S.T. Nguyen, R.S. Ruoff, Preparation and characterization of graphene oxide paper, Nature 448 (2007) 457–460, doi:10.1038/nature06016.

[18] Z. Ling, C.E. Ren, M.Q. Zhao, J. Yang, J.M. Giammarco, J. Qiu, M.W. Barsoum, Y. Gogotsi, Flexible and conductive MXene films and nanocomposites with high capacitance, in: Proc. Natl. Acad. Sci. U. S. A., 111, 2014, pp. 16676–16681, doi:10.1073/pnas.1414215111.

[19] B. Shen, W. Zhai, W. Zheng, Ultrathin flexible graphene film: an excellent thermal conducting material with efficient EMI shielding, Adv. Funct. Mater. 24 (2014) 4542–4548, doi:10.1002/adfm.201400079.

[20] Z.L. Ma, S.L. Kang, J.Z. Ma, L. Shao, Y.L. Zhang, C. Liu, A.J. Wei, X.L. Xiang, L.F. Wei, J.W. Gu, Ultraflexible and mechanically strong double-layered aramid nanofiber-$Ti_3C_2T_x$ MXene/silver nanowire nanocomposite papers for high-performance electromagnetic interference shielding, ACS Nano 14 (2020) 8368–8382, doi:10.1021/acsnano.0c02401.

[21] W.T. Cao, F.F. Chen, Y.J. Zhu, Y.G. Zhang, Y.Y. Jiang, M.G. Ma, F. Chen, Binary strengthening and toughening of MXene/Cellulose nanofiber composite paper with nacre-inspired structure and superior electromagnetic interference shielding properties, ACS Nano 12 (2018) 4583–4593, doi:10.1021/acsnano.8b00997.

[22] S. Wan, X. Li, Y. Chen, N. Liu, Y. Du, S. Dou, L. Jiang, Q. Cheng, High-strength scalable MXene films through bridging-induced densification, Science 374 (2021) 96–99, doi:10.1126/science.abg2026.

[23] S. Wan, Y. Chen, Y. Wang, G. Li, G. Wang, L. Liu, J. Zhang, Y. Liu, Z. Xu, A.P. Tomsia, L. Jiang, Q. Cheng, Ultrastrong graphene films via long-chain π-bridging, Matter 1 (2019) 389–401, doi:10.1016/j.matt.2019.04.006.

[24] T. Kuila, S. Bose, C.E. Hong, M.E. Uddin, P. Khanra, N.H. Kim, J.H. Lee, Preparation of functionalized graphene/linear low density polyethylene composites by a solution mixing method, Carbon 49 (2011) 1033–1037, doi:10.1016/j.carbon.2010.10.031.

[25] H. Wang, G. Xie, M. Fang, Z. Ying, Y. Tong, Y. Zeng, Mechanical reinforcement of graphene/poly(vinyl chloride) composites prepared by combining the in-situ suspension polymerization and melt-mixing methods, Compos. Part B-Eng. 113 (2017) 278–284, doi:10.1016/j.compositesb.2017.01.053.

[26] A.S. Patole, S.P. Patole, H. Kang, J.-B. Yoo, T.-H. Kim, J.-H. Ahn, A facile approach to the fabrication of graphene/polystyrene nanocomposite by in situ microemulsion polymerization, J. Colloid Interface Sci. 350 (2010) 530–537, doi:10.1016/j.jcis.2010.01.035.

[27] U.G.K. Wegst, H. Bai, E. Saiz, A.P. Tomsia, R.O. Ritchie, Bioinspired structural materials, Nat. Mater. 14 (2015) 23–36, doi:10.1038/nmat4089.

[28] J. Peng, Q. Cheng, High-performance nanocomposites inspired by nature, Adv. Mater. 29 (2017) 1702959, doi:10.1002/adma.201702959.

[29] F. Barthelat, Z. Yin, M.J. Buehler, Structure and mechanics of interfaces in biological materials, Nat. Rev. Mater. 1 (2016) 16007, doi:10.1038/natrevmats.2016.7.

[30] C. Sanchez, H. Arribart, M.M.G. Guille, Biomimetism and bioinspiration as tools for the design of innovative materials and systems, Nat. Mater. 4 (2005) 277–288, doi:10.1038/nmat1339.

[31] T. Zhou, H. Ni, Y. Wang, C. Wu, H. Zhang, J. Zhang, A.P. Tomsia, L. Jiang, Q. Cheng, Ultratough graphene-black phosphorus films, in: Proc. Natl. Acad. Sci. U. S. A., 117, 2020, pp. 8727–8735, doi:10.1073/pnas.1916610117.

[32] C. Wu, T. Zhou, Y. Du, S. Dou, H. Zhang, L. Jiang, Q. Cheng, Strong bioinspired HPA-rGO nanocomposite films via interfacial interactions for flexible supercapacitors, Nano Energy 58 (2019) 517–527, doi:10.1016/j.nanoen.2019.01.055.

[33] P. Ming, Z. Song, S. Gong, Y. Zhang, J. Duan, Q. Zhang, L. Jiang, Q. Cheng, Nacre-inspired integrated nanocomposites with fire retardant properties by graphene oxide and montmorillonite, J. Mater. Chem. A 3 (2015) 21194–21200, doi:10.1039/c5ta05742f.

[34] S. Wan, S. Fang, L. Jiang, Q. Cheng, R.H. Baughman, Strong, conductive, foldable graphene sheets by sequential ionic and pi bridging, Adv. Mater. 30 (2018) 1802733, doi:10.1002/adma.201802733.

[35] F. Shahzad, M. Alhabeb, C.B. Hatter, B. Anasori, S. Man Hong, C.M. Koo, Y. Gogotsi, Electromagnetic interference shielding with 2D transition metal carbides (MXenes), Science 353 (2016) 1137–1140, doi:10.1126/science.aag2421.

[36] T. Zhou, C. Wu, Y. Wang, A.P. Tomsia, M. Li, E. Saiz, S. Fang, R.H. Baughman, L. Jiang, Q. Cheng, Super-tough MXene-functionalized graphene sheets, Nat. Commun. 11 (2020) 2077, doi:10.1038/s41467-020-15991-6.

[37] J. Zhang, N. Kong, S. Uzun, A. Levitt, S. Seyedin, P.A. Lynch, S. Qin, M. Han, W. Yang, J. Liu, X. Wang, Y. Gogotsi, J.M. Razal, Scalable manufacturing of free-standing, strong $Ti_3C_2T_x$ MXene films with outstanding conductivity, Adv. Mater. 32 (2020) 2001093, doi:10.1002/adma.202001093.

[38] Y. Li, B. Zhou, Y. Shen, C. He, B. Wang, C. Liu, Y. Feng, C. Shen, Scalable manufacturing of flexible, durable $Ti_3C_2T_x$ MXene/Polyvinylidene fluoride film for multifunctional electromagnetic interference shielding and electro/photo-thermal conversion applications, Compos. Part B-Eng. 217 (2021) 108902, doi:10.1016/j.compositesb.2021.108902.

[39] J. Lipton, J.A. Röhr, V. Dang, A. Goad, K. Maleski, F. Lavini, M. Han, E.H.R. Tsai, G.-M. Weng, J. Kong, E. Riedo, Y. Gogotsi, A.D. Taylor, Scalable, highly conductive, and micropatternable MXene films for enhanced electromagnetic interference shielding, Matter 3 (2020) 546–557, doi:10.1016/j.matt.2020.05.023.

[40] G.M. Weng, J. Li, M. Alhabeb, C. Karpovich, H. Wang, J. Lipton, K. Maleski, J. Kong, E. Shaulsky, M. Elimelech, Y. Gogotsi, A.D. Taylor, Layer-by-layer assembly of cross-functional semi-transparent MXene-carbon nanotubes composite films for next-generation electromagnetic interference shielding, Adv. Funct. Mater. 28 (2018) 1803360, doi:10.1002/adfm.201803360.

[41] J. Song, C. Chen, Y. Zhang, High thermal conductivity and stretchability of layer-by-layer assembled silicone rubber/graphene nanosheets multilayered films, Compos. Part A Appl. Sci. Manuf. 105 (2018) 1–8, doi:10.1016/j.compositesa.2017.11.001.

[42] X. Zhang, Y. Guo, Y. Liu, Z. Li, W. Fang, L. Peng, J. Zhou, Z. Xu, C. Gao, Ultrathick and highly thermally conductive graphene films by self-fusion, Carbon 167 (2020) 249–255, doi:10.1016/j.carbon.2020.05.051.

[43] X. Zhong, D. Wang, J. Sheng, Z. Han, C. Sun, J. Tan, R. Gao, W. Lv, X. Xu, G. Wei, X. Zou, G. Zhou, Freestanding and sandwich MXene-based cathode with suppressed lithium polysulfides shuttle for flexible lithium-sulfur batteries, Nano Lett 22 (2022) 1207–1216, doi:10.1021/acs.nanolett.1c04377.

[44] J.J. Richardson, M. Bjornmalm, F. Caruso, Multilayer assembly. Technology-driven layer-by-layer assembly of nanofilms, Science 348 (2015) aaa2491, doi:10.1126/science.aaa2491.

[45] S. Wan, J. Peng, Y. Li, H. Hu, L. Jiang, Q. Cheng, Use of synergistic interactions to fabricate strong, tough, and conductive artificial nacre based on graphene oxide and chitosan, ACS Nano 9 (2015) 9830–9836, doi:10.1021/acsnano.5b02902.

[46] S. Wan, F. Xu, L. Jiang, Q. Cheng, Superior fatigue resistant bioinspired graphene-based nanocomposite via synergistic interfacial interactions, Adv. Funct. Mater. 27 (2017) 1605636, doi:10.1002/adfm.201605636.

[47] S. Wan, Q. Zhang, X. Zhou, D. Li, B. Ji, L. Jiang, Q. Cheng, Fatigue resistant bioinspired composite from synergistic two-dimensional nanocomponents, ACS Nano 11 (2017) 7074–7083, doi:10.1021/acsnano.7b02706.

[48] S. Gong, Q. Zhang, R. Wang, L. Jiang, Q. Cheng, Synergistically toughening nacre-like graphene nanocomposites via gel-film transformation, J. Mater. Chem. A 5 (2017) 16386–16392, doi:10.1039/c7ta03535g.

[49] H. Ni, F. Xu, A.P. Tomsia, E. Saiz, L. Jiang, Q. Cheng, Robust bioinspired graphene film via pi-pi cross-linking, ACS Appl. Mater. Interface. 9 (2017) 24987–24992, doi:10.1021/acsami.7b07748.

[50] Q. Cheng, M. Wu, M. Li, L. Jiang, Z. Tang, Ultratough artificial nacre based on conjugated cross-linked graphene oxide, Angew. Chem. Int. Ed. 52 (2013) 3750–3755, doi:10.1002/anie.201210166.

[51] R. Xiong, K. Hu, A.M. Grant, R. Ma, W. Xu, C. Lu, X. Zhang, V.V. Tsukruk, Ultrarobust transparent cellulose nanocrystal-graphene membranes with high electrical conductivity, Adv. Mater. 28 (2016) 1501–1509, doi:10.1002/adma. 201504438.

[52] Y. Cheng, J. Peng, H. Xu, Q. Cheng, Glycera-inspired synergistic interfacial interactions for constructing ultrastrong graphene-based nanocomposites, Adv. Funct. Mater. 28 (2018) 1800924, doi:10.1002/adfm.201800924.

[53] P. Song, Z. Xu, Y. Wu, Q. Cheng, Q. Guo, H. Wang, Super-tough artificial nacre based on graphene oxide via synergistic interface interactions of pi-pi stacking and hydrogen bonding, Carbon 111 (2017) 807–812, doi:10.1016/j.carbon.2016. 10.067.

[54] S. Wan, Y. Li, J. Peng, H. Hu, Q. Cheng, L. Jiang, Synergistic toughening of graphene oxide-molybdenum disulfide-thermoplastic polyurethane ternary artificial nacre, ACS Nano 9 (2015) 708–714, doi:10.1021/nn506148w.

[55] P. Li, Y. Yang, Y. Liu, H. Qin, J. Liu, Z. Xu, Y. Liu, F. Meng, J. Lin, F. Wang, C. Gao, Continuous crystalline graphene papers with gigapascal strength by intercalation modulated plasticization, Nat. Commun. 11 (2020) 2645, doi:10. 1038/s41467-020-16494-0.

[56] Q. Wei, S. Pei, X. Qian, H. Liu, Z. Liu, W. Zhang, T. Zhou, Z. Zhang, X. Zhang, H.M. Cheng, W. Ren, Superhigh electromagnetic interference shielding of ultrathin aligned pristine graphene nanosheets film, Adv. Mater. 32 (2020) 1907411, doi:10.1002/adma.201907411.

[57] S. Wan, Y. Chen, S. Fang, S. Wang, Z. Xu, L. Jiang, R.H. Baughman, Q. Cheng, High-strength scalable graphene sheets by freezing stretch-induced alignment, Nat. Mater. 20 (2021) 624–631, doi:10.1038/s41563-020-00892-2.

[58] A. Akbari, B.V. Cunning, S.R. Joshi, C. Wang, D.C. Camacho-Mojica, S. Chatterjee, V. Modepalli, C. Cahoon, C.W. Bielawski, P. Bakharev, G.-H. Kim, R.S. Ruoff, Highly Ordered and Dense Thermally conductive graphitic films from a graphene oxide/reduced graphene oxide mixture, Matter 2 (2020) 1198–1206, doi:10.1016/ j.matt.2020.02.014.

[59] Y. Zhang, S. Wang, P. Tang, Z. Zhao, Z. Xu, Z.Z. Yu, H.B. Zhang, Realizing spontaneously regular stacking of pristine graphene oxide by a chemical-structure-engineering strategy for mechanically strong macroscopic films, ACS Nano 16 (2022) 8869–8880, doi:10.1021/acsnano.1c10561.

[60] S. Wan, X. Li, Y. Wang, Y. Chen, X. Xie, R. Yang, A.P. Tomsia, L. Jiang, Q. Cheng, Strong sequentially bridged MXene sheets, in: Proc. Natl. Acad. Sci. U. S. A., 117, 2020, pp. 27154–27161, doi:10.1073/pnas.2009432117.

[61] J. Lipton, G.M. Weng, M. Alhabeb, K. Maleski, F. Antonio, J. Kong, Y. Gogotsi, A.D. Taylor, Mechanically strong and electrically conductive multilayer MXene nanocomposites, Nanoscale 11 (2019) 20295–20300, doi:10.1039/c9nr06015d.

[62] W. Cao, C. Ma, S. Tan, M. Ma, P. Wan, F. Chen, Ultrathin and flexible CNTs/MXene/cellulose nanofibrils composite paper for electromagnetic interference shielding, Nanomicro Lett. 11 (2019) 72, doi:10.1007/ s40820-019-0304-y.

[63] Z. Zhan, Q. Song, Z. Zhou, C. Lu, Ultrastrong and conductive MXene/cellulose nanofiber films enhanced by hierarchical nano-architecture and interfacial interaction for flexible electromagnetic interference shielding, J. Mater. Chem. C 7 (2019) 9820–9829, doi:10.1039/c9tc03309b.

[64] H. Chen, Y. Wen, Y. Qi, Q. Zhao, L. Qu, C. Li, Pristine titanium carbide MXene films with environmentally stable conductivity and superior mechanical strength, Adv. Funct. Mater. 30 (2019) 1906996, doi:10.1002/adfm.201906996.

[65] R. Liu, M. Miao, Y. Li, J. Zhang, S. Cao, X. Feng, Ultrathin biomimetic polymeric $Ti_3C_2T_x$ MXene composite films for electromagnetic interference shielding, ACS Appl. Mater. Interface. 10 (2018) 44787–44795, doi:10.1021/acsami.8b18347.

[66] Z. Liu, Y. Zhang, H.-B. Zhang, Y. Dai, J. Liu, X. Li, Z.-Z. Yu, Electrically conductive aluminum ion-reinforced MXene films for efficient electromagnetic interference shielding, J. Mater. Chem. C 8 (2020) 1673–1678, doi:10.1039/c9tc06304h.

[67] G.S. Lee, T. Yun, H. Kim, I.H. Kim, J. Choi, S.H. Lee, H.J. Lee, H.S. Hwang, J.G. Kim, D.W. Kim, H.M. Lee, C.M. Koo, S.O. Kim, Mussel inspired highly aligned $Ti_3C_2T_x$ MXene film with synergistic enhancement of mechanical strength and ambient stability, ACS Nano 14 (2020) 11722–11732, doi:10.1021/acsnano.0c04411.

[68] P. Li, Y. Han, M. Wang, X. Cao, J. Gao, Y. Liu, X. Chen, B. Wang, B. Wang, C. Zhu, X. Wang, K. Cao, M. Huang, B.V. Cunning, J. Pang, W. Xu, Y. Ying, Z. Xu, W. Fang, Y. Lu, R.S. Ruoff, C. Gao, Multifunctional macroassembled graphene nanofilms with high crystallinity, Adv. Mater. 33 (2021) 2104195, doi:10.1002/ adma.202104195.

[69] X.H. Zha, J. Zhou, Y. Zhou, Q. Huang, J. He, J.S. Francisco, K. Luo, S. Du, Promising electron mobility and high thermal conductivity in Sc_2CT_2 (T = F, OH) MXenes, Nanoscale 8 (2016) 6110–6117, doi:10.1039/c5nr08639f.

[70] L. Li, Y. Cao, X. Liu, J. Wang, Y. Yang, W. Wang, Multifunctional MXene-based fireproof electromagnetic shielding films with exceptional anisotropic heat dissipation capability and Joule heating performance, ACS Appl. Mater. Interface. 12 (2020) 27350–27360, doi:10.1021/acsami.0c05692.

[71] X. Jin, J. Wang, L. Dai, X. Liu, L. Li, Y. Yang, Y. Cao, W. Wang, H. Wu, S. Guo, Flame-retardant poly(vinyl alcohol)/MXene multilayered films with outstanding electromagnetic interference shielding and thermal conductive performances, Chem. Eng. J. 380 (2020) 122475, doi:10.1016/j.cej.2019.122475.

[72] B. Zhou, Q. Li, P. Xu, Y. Feng, J. Ma, C. Liu, C. Shen, An asymmetric sandwich structural cellulose-based film with self-supported MXene and AgNW layers for flexible electromagnetic interference shielding and thermal management, Nanoscale 13 (2021) 2378–2388, doi:10.1039/d0nr07840a.

[73] Y. Liu, K. Wu, M. Lu, E. Jiao, H. Zhang, J. Shi, M. Lu, Highly thermal conductivity and flame retardant flexible graphene/MXene paper based on an optimized interface and nacre laminated structure, Compos. Part A Appl. Sci. Manuf. 141 (2021) 106227, doi:10.1016/j.compositesa.2020.106227.

[74] P. Kumar, F. Shahzad, S. Yu, S.M. Hong, Y.-H. Kim, C.M. Koo, Large-area reduced graphene oxide thin film with excellent thermal conductivity and electromagnetic interference shielding effectiveness, Carbon 94 (2015) 494–500, doi:10.1016/j.carbon.2015.07.032.

[75] J. Xi, J. Li, E. Zhou, Y. Liu, W. Gao, Y. Guo, J. Ying, Z. Chen, G. Chen, C. Gao, Graphene aerogel films with expansion enhancement effect of high-performance electromagnetic interference shielding, Carbon 135 (2018) 44–51, doi:10.1016/j. carbon.2018.04.041.

[76] T. Yun, H. Kim, A. Iqbal, Y.S. Cho, G.S. Lee, M.K. Kim, S.J. Kim, D. Kim, Y. Gogotsi, S.O. Kim, C.M. Koo, Electromagnetic shielding of monolayer MXene assemblies, Adv. Mater. 32 (2020) 1906769, doi:10.1002/adma.201906769.

[77] J. Liu, H.B. Zhang, R. Sun, Y. Liu, Z. Liu, A. Zhou, Z.Z. Yu, Hydrophobic, Flexible, and lightweight MXene foams for high-performance electromagnetic-interference shielding, Adv. Mater. 29 (2017) 1702367, doi:10.1002/adma. 201702367.

[78] W. Chen, L.X. Liu, H.B. Zhang, Z.Z. Yu, Kirigami-inspired highly stretchable, conductive, and hierarchical $Ti_3C_2T_x$ MXene films for efficient electromagnetic interference shielding and pressure sensing, ACS Nano 15 (2021) 7668–7681, doi:10.1021/acsnano.1c01277.

[79] J. Liu, Z. Liu, H.B. Zhang, W. Chen, Z. Zhao, Q.W. Wang, Z.Z. Yu, Ultrastrong and highly conductive MXene-based films for high-performance electromagnetic interference shielding, Adv. Electron. Mater. 6 (2019) 1901094, doi:10.1002/aelm. 201901094.

Review